Fields at Work GmbH, Hegibachstrasse 41, 8032 Zürich, Schweiz
Tel. +41 (44) 382 38 31
info@fieldsatwork.ch
www.fieldsatwork.ch

FSM-DENMACHEN (Project C2018-01)

Final Report

October 2023

Authors: Marco Zahner, Fabian Schneider, Jürg Fröhlich

Table of Contents

Fields at Work GmbH, Hegibachstrasse 41, 8032 Zürich, Schweiz
Tel. +41 (44) 382 38 31
info@fieldsatwork.ch
www.fieldsatwork.ch

Fields at Work GmbH, Hegibachstrasse 41, 8032 Zürich, Schweiz
Tel. +41 (44) 382 38 31
info@fieldsatwork.ch
www.fieldsatwork.ch

Introduction

1.1 Background & Motivation

Concerns about potential health effects from electromagnetic field exposure are still common in the Swiss population and worldwide, which is one of the reasons why the Swiss parliament has requested to install a nationwide monitoring of the RF-EMF exposure which is currently being implemented. This monitoring aims to capture all the contributions of everyday immissions, mainly caused by fixed installations such as the mobile communication and broadcasting infrastructure. The contribution of the user equipment is not covered by this approach, though. EMF exposure caused by the emissions of the own mobile devices can represent a substantial share in the overall RF-EMF exposure dose of a person. Smartphones for example are carried close to the body for extended periods of time. Although a phone might only be actively transmitting sporadically and for short periods of time, the electromagnetic fields in proximity of the device can reach values that are several orders of magnitude stronger than any contribution of the much more distant transmitters of the fixed infrastructure (far field exposure) during these short active transmission phases. Depending on individual device usage and circumstances, the emissions from the own device can even represent the biggest share of the total RF-EMF exposure dose. There are several factors that make it challenging to quantify near-field contributions. Compared to far-field exposure, near field exposure is much more variable over time and depends to a very large extent on the individual behavior. The exposure is not only influenced by how and where a device is used but also by the endless customization options allowed by a modern smartphone and its background data transmission activity. The issue is further aggravated by the increasing complexity and dynamicity of modern telecommunication standards. The lack of suitable direct measurement tools forced epidemiological studies to rely on proxies covering these contributions of the exposure and is therefore affected by high uncertainties. Furthermore, little data is available about the output power of mobile phones in the 4G and 5G networks in real life situations. The SAR value determined by the manufacturers is based on standardized worst-case scenarios with limited practical relevance.

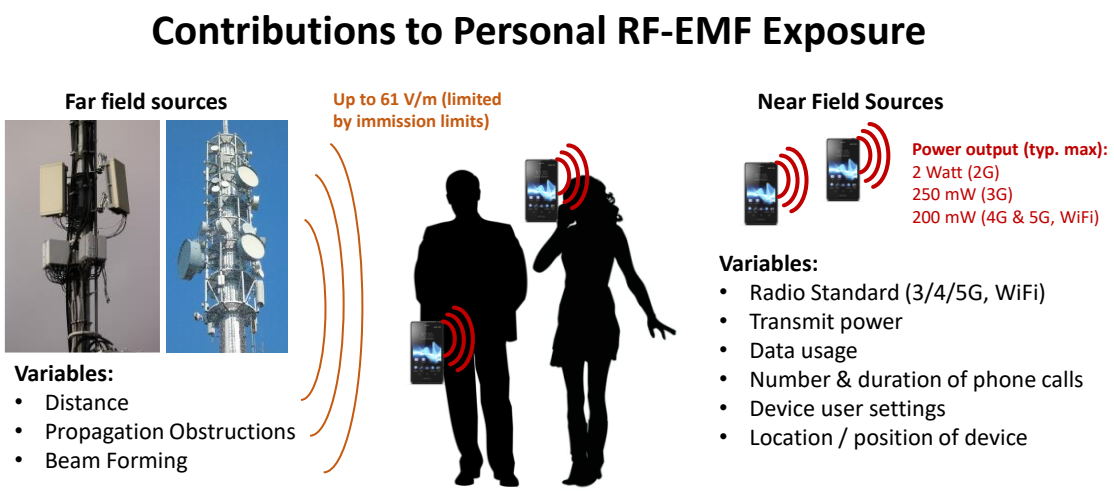

Various tools and methods have been proposed for the epidemiological assessment of near field sources. These include questionnaires, smartphone-app-based approaches, operator data analysis. However, these

approaches suffer either from high uncertainty and/or various practical limitations. As an example, attempts to use the smartphone to assess uplink activity fail due to the very restricted access to relevant operational parameters by standard smartphone apps.

1.2 Objectives

This project aims to develop a novel adhesive patch for the skin. This flexible planar device integrates field probes with RF detector electronics for measuring the radiofrequency electric field strength (RF-EMF) from close-to-body mobile devices directly on the skin. The field strength shall be measured at several locations which are known or expected to be subjected to elevated EMF levels such as around the ear. The objective is to provide a tool which allows to significantly reduce the current uncertainty for the assessment of the contribution of near-field sources to the total RF-EMF exposure in everyday situations.

1.3 Design and Implementation Requirements

1.3.1 General requirements

To be suitable for the intended use, the measurement patch must fulfil several basic requirements. Small size and low weight are crucial characteristics for a wearable device. This poses strict battery size limits and implies a correspondingly low power consumption of the device. From an electrical point of view, the measurement device needs to be wideband to cover at least all telecommunication frequency bands in the range from 700 MHz to 6 GHz and sensitive to arbitrarily oriented electric field vectors (including the orientation perpendicular to the skin). The device must feature sufficient on-board memory to enable long-term measurements with high temporal resolution. The device must also be easy to use to an extent that allows uninformed people to power it on and off and determine its state of operation without the need for an expert to be present.

1.3.2 Measurement quantity and accuracy

A crucial question in the context of the patch development is the definition of the actual quantity that should be measured by the patch. The goal of the approach is to measure the exposure of the subjects to near-field EMF radiation. Ideally, the measurement value will provide a low-uncertainty proxy for the estimation of the SAR value experienced by the subject. This means that the measurement of interest must mostly take place in the near-field region of a transmitting mobile phone antenna. Unlike far-field radiation, near-fields are characterized by having no well-defined relationship between electrical and magnetic field component. Furthermore, the field strength is inherently very location dependent, exhibits localized hotspots, and falls off very quickly with distance. Large variations can occur even within fractions of a wavelength at telecommunication frequencies. The measurement probe must therefore be as small as possible and disturb the field distribution as little as possible. This can be achieved using an electrically small, high-impedance E-field probe. The electrical field strength will be the measurement quantity in the focus of this project.

In contrast to automated standardized SAR value assessments, neither the instantaneous output power of the EMF source nor the relative position of the source and measurement point are exactly known. To maximize the probability to take a measurement at the spot of highest exposure, several measurement points per location are therefore required. In this context, it makes sense to prioritize a higher number of measurement points over absolute accuracy and complexity of the individual sensors.

Fields at Work GmbH, Hegibachstrasse 41, 8032 Zürich, Schweiz
Tel. +41 (44) 382 38 31
info@fieldsatwork.ch
www.fieldsatwork.ch

2 Development of the Device

2.1 Overall concept and exposure assessment approach

The proposed overall personal exposure assessment concept using the novel device is shown schematically in Figure 1. This project investigates a new measurement approach consisting of a hybrid near- and far field sensor setup. A set of miniature, wearable field probes (represented as yellow stars in the figure) is used to monitor the local field strength at selected locations on the body. These field probes are as small and lightweight as possible and dedicated to the assessment nearfield contributions and strong far field contributions.

Figure 1: Personal exposure assessment concept using the sensor patch: Nearfield measurements at strategic locations (yellow stars) are complemented by portable exposimeter measurements (red box).

The small size of the field probes sets limits on the achievable sensitivity and selectivity of the measurement. For this reason, the nearfield measurements are complemented by exposure meter measurements taking place simultaneously. The role of the exposimeter in this concept is twofold: It provides accurate far-field data with the sensitivity and a high dynamic range that the patch sensor is not able to provide. In addition, the exposimeter data can be used to classify the exposure events assessed by the on-body field probes and provide auxiliary information. A strong emission from an on-body device is likely to be captured by both the patch sensor and the exposimeter. The patch sensor can focus on the assessment of the amplitude and time pattern of the field strength whereas the exposimeter is used to identify the frequency and possible wireless technology of the source.

2.2 RF Detectors

2.2.1 Technology evaluation

The very restricted power and energy budget calls for a very low-power measurement method. The objective After considering various technologies we opted for a diode-based detector approach. A diode detector has several characteristics which are interesting for this project, the most obvious one being the fact that it is completely passive. A diode detector directly converts a high frequency signal into a proportional (tiny) DC voltage without the need of any power supply or auxiliary RF electronics.

Advantages	Drawbacks
• Fully passive (zero power consumption) • Minimal component count • Very small size possible • High measurement impedance • Wideband frequency response	• Limited dynamic range • Response time vs. noise trade-off • No frequency selectivity • Semiconductor temperature drift

Table 1: General properties of diode-based detectors

This detector technology has also its downsides of course. The most important challenges are a limited dynamic range, worse sensitivity and higher proneness to temperature drift issues compared to approaches using active components. However, many of these shortcomings are be offset by the hybrid measurement concept explained in section 2.1.

2.2.2 Isolation of detectors (High-Z lines)

The presence of the measurement device must influence the near field as little as possible. The presence of metallic objects and thick dielectric parts in the measurement spot must therefore be kept to a minimum. The diode detector itself can be made very small but the tiny output signal must be amplified and digitized at some point to avoid signal degradation. A special electrical connection is therefore required to physically isolate the small RF detectors from the readout electronics. This connection must be as transparent to the local electromagnetic field as possible in order not to disturb the field distribution at the measurement location. However, some form of electrical connection is still required to retrieve the measurement values. This can be achieved using high resistivity connections. Such connections can be implemented using carbon tracks or other materials which would however require to rely on non-standard fabrication processes. We therefore decided to realize the high resistance line using discrete components, i.e., a string of connected resistors instead of a continuous high-resistivity trace material. Electromagnetic simulations have been carried out to determine the minimum required resistivity and spacing between the resistors to achieve the desired effect.

Fields at Work GmbH, Hegibachstrasse 41, 8032 Zürich, Schweiz
Tel. +41 (44) 382 38 31
info@fieldsatwork.ch
www.fieldsatwork.ch

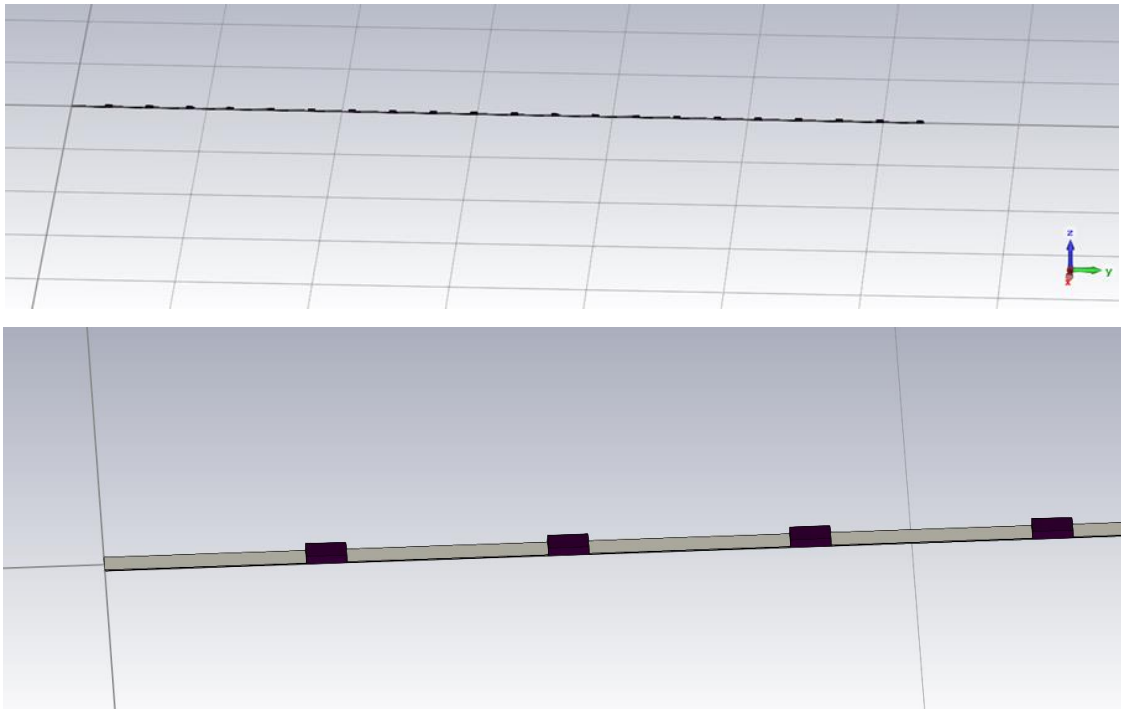

Figure 2: Electromagnetic simulation model of a high resistance line realized with discrete resistive elements.

A high resistance line (10 cm length) composed of a string of 20 resistors was exposed to a plane wave in the frequency range from 400 MHz to 5800 MHz. The resistor values were increased until no obvious disturbance of the plane could be observed. A value of 10 kΩ per resistor was determined experimentally to be adequate for the purpose. The following pictures show a comparison of the resulting local RMS field strength for a way too low resistance value (like a direct connection) and the chosen value of 10 kΩ.

Fields at Work GmbH, Hegibachstrasse 41, 8032 Zürich, Schweiz
Tel. +41 (44) 382 38 31
info@fieldsatwork.ch
www.fieldsatwork.ch

Freq.	Resistance per element = 1 Ohm	Resistance per element = 10k Ohm
400 MHz	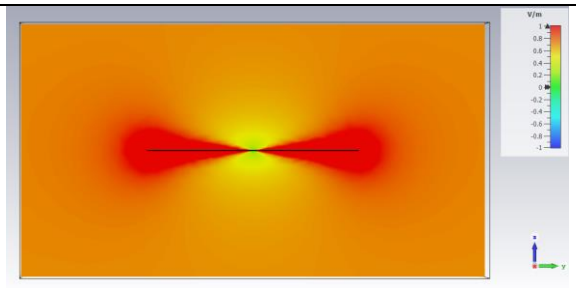	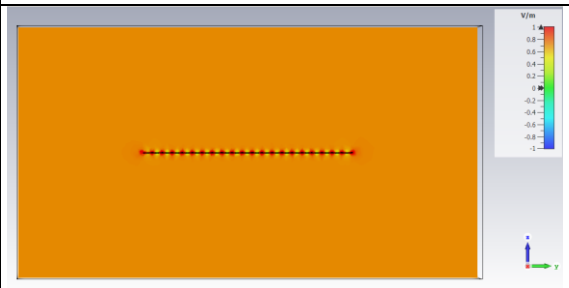
900 MHz	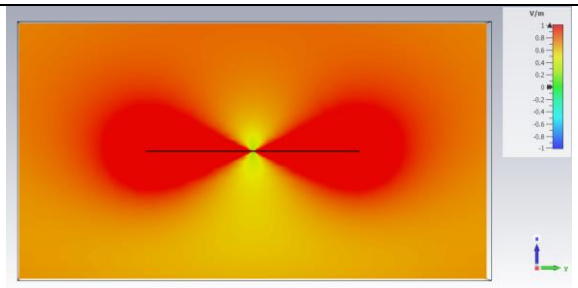	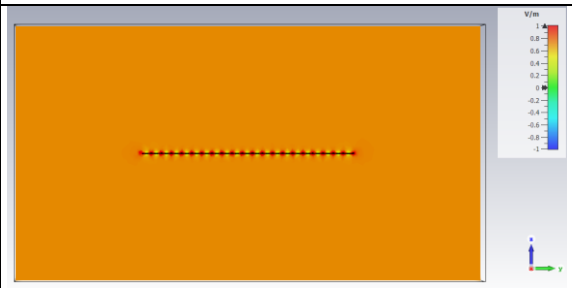
1.8 GHz	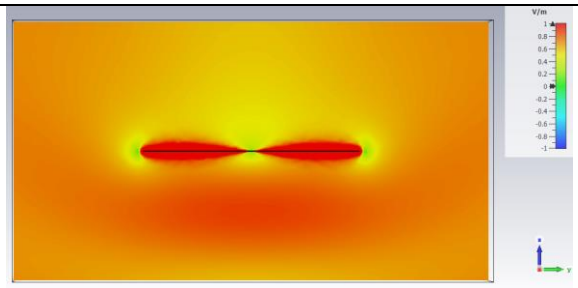	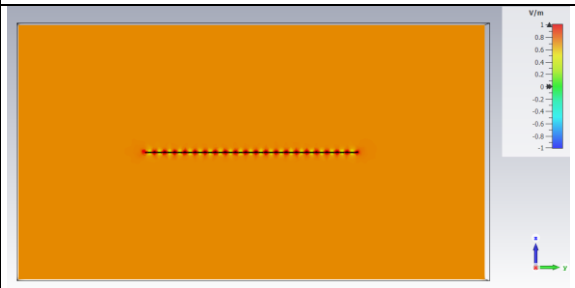
3.5 GHz	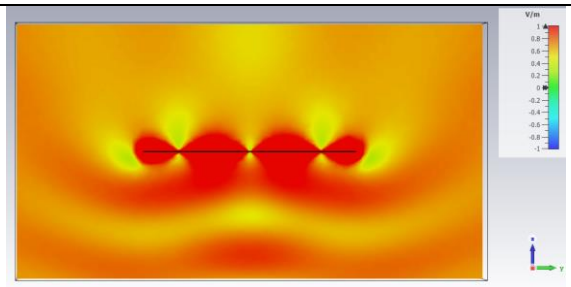	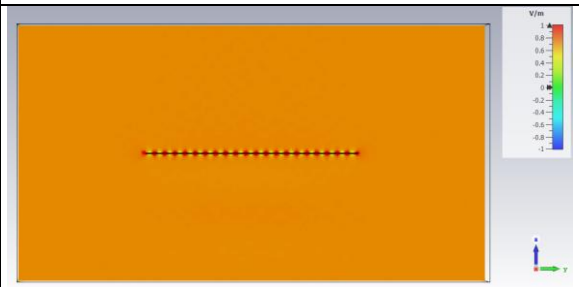
5.8 GHz	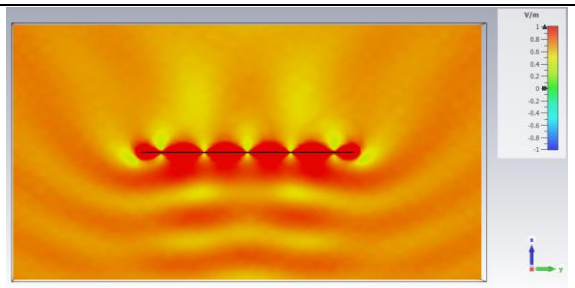	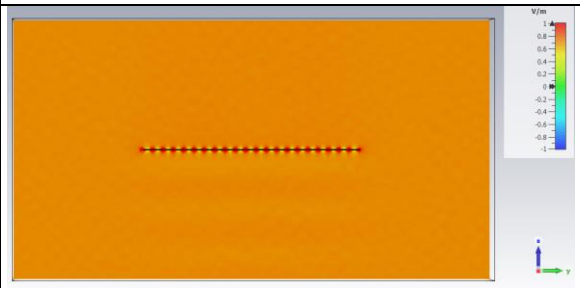

Figure 3: Simulation results (CST Studio); Influence of the high resistance line on an impinging plane wave at various frequencies (RMS values shown). The proposed discrete 10 kΩ resistor string is virtually transparent to the EMF.

Fields at Work GmbH, Hegibachstrasse 41, 8032 Zürich, Schweiz
Tel. +41 (44) 382 38 31
info@fieldsatwork.ch
www.fieldsatwork.ch

2.3 Iterations and Performance evaluations

2.3.1 Diode detector performance in a 50 Ohm environment

Laboratory tests to evaluate the feasibility of the fully passive RF detection approach in terms of dynamic range and frequency response were performed. A test PCB implementing a passive diode detector was designed and manufactured. It consists of a detector diode connected in parallel to a terminated 50 Ohm transmission line. The diode that has been selected for this test is a low barrier microwave Schottky diode in a tiny chip scale package. It is therefore well suited for a miniaturized patch implementation. In this measurement the response of the detector over the frequency range of interest (100 MHz to 5800 MHz) was performed for different input power levels. The results are shown in Figure 4.

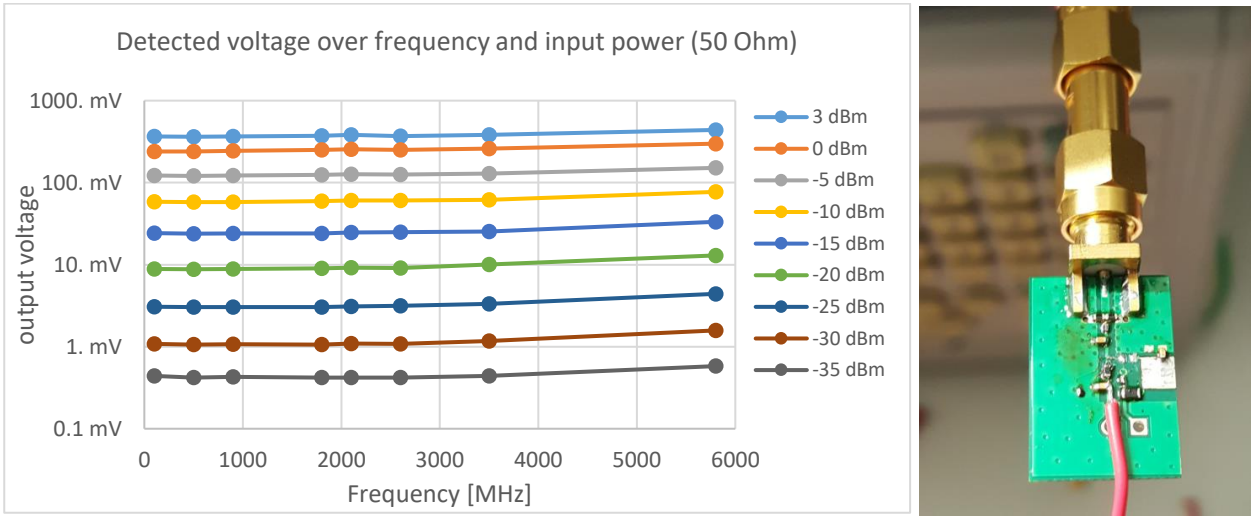

Figure 4: Measured bandwidth and dynamic range of a fully passive detector using a low barrier microwave Schottky diode. Right: custom test board and measurement setup.

The measurement shows that this detector approach features a very flat frequency response over the whole sub-6 GHz communication frequency range. It is also easily able to cover a dynamic range of 35 dB while featuring an output voltage proportional to the incident power over most of the measurement range (square-law region). This makes this kind of detector inherently a power sensor with a response proportional to the RMS value of the input signal. The addition of a low-power amplification stage between the detector output and the analog to digital converter (ADC) for signals below 1 mV should provide an additional 5-15 dB useable dynamic range at the low end of the measurement range. However, these numbers cannot be directly transferred to the final setting as latter will consist in an environment with much higher impedance (E-Field probe) compared to the 50 Ohm environment of the test.

The choice of a different detector diode, such as a zero-bias Schottky RF detector is another degree of freedom which was investigated. Zero-bias Schottky diodes provide a higher sensitivity when used in an unbiased configuration, might however suffer from a higher temperature drift than their low-barrier height counterparts. At this stage it is difficult to determine how much a temperature drift of the diodes might affect the result of the final sensor patch, though.

2.3.2 Evaluation of the field probe configuration

The next step was to determine how the characteristics of the detector are affected when moving from a 50 Ohm environment to a field probe configuration. The field probe configuration consists of connecting

Fields at Work GmbH, Hegibachstrasse 41, 8032 Zürich, Schweiz
Tel. +41 (44) 382 38 31
info@fieldsatwork.ch
www.fieldsatwork.ch

the detector directly to an (as short as possible) metal pin to directly pick up the electric field component by means of capacitive coupling. One of the challenges consists in finding the best trade-off between mechanical size and sensitivity of the field probe. The sorter the pin, the lower the amount of charge which is displaced by the external electric field. The performance in this high-impedance environment does largely depend on the intrinsic properties of the detector diode, especially the threshold voltage and junction capacitance. A prototype on a standard printed circuit board was therefore designed to evaluate the performance of different RF diode models in this detector configuration (Figure 5).

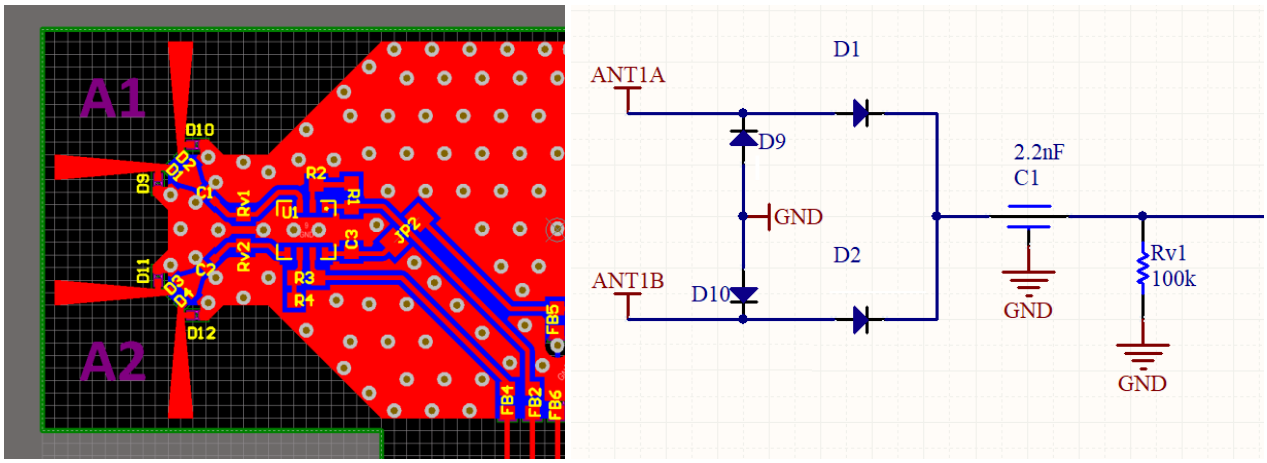

Figure 5: Layout of the diode evaluation board for the field probe configuration (left). Schematic of one detector element (right).

Four detector elements are arranged on the test board (one per corner) each of which consists of a pair of orthogonally arranged field probes with a length of 4 mm, whose voltages are combined to be sensitive to two field polarizations. The field probe was evaluated in the anechoic chamber. The measurement setup is shown in Figure 6. This setup allows to apply field strengths of well defined and controlled amplitude and polarization as the main goal of this evaluation was the comparison of different electronic components.

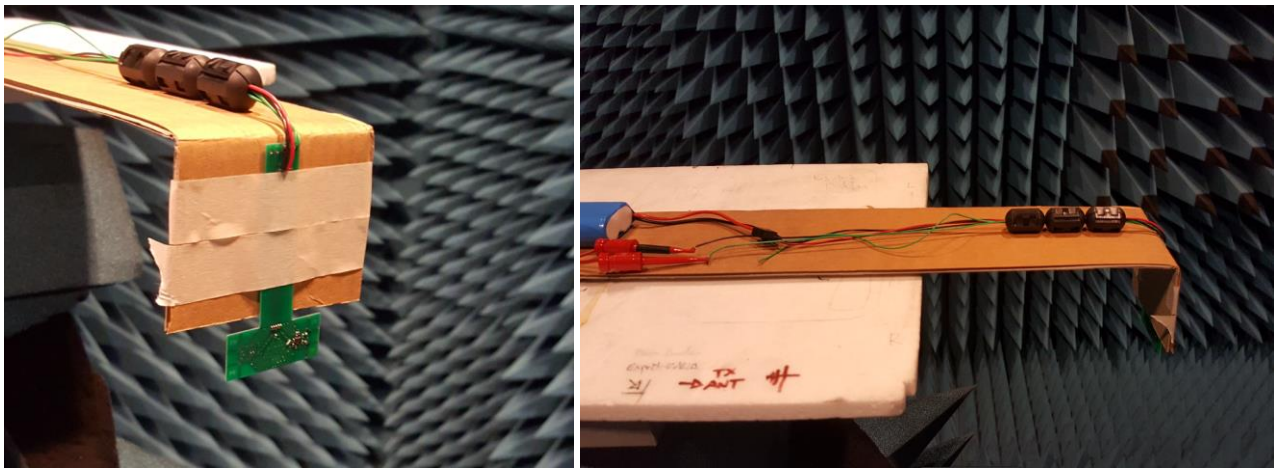

Figure 6: Measurement setup in the anechoic chamber for the evaluation of various diodes in field probe configuration.

From the test results we could draw following conclusions:

Fields at Work GmbH, Hegibachstrasse 41, 8032 Zürich, Schweiz
Tel. +41 (44) 382 38 31
info@fieldsatwork.ch
www.fieldsatwork.ch

- A probe length of just 4 mm, when combined with a large ground plane and a suitable detector diode, is enough to provide a usable output voltage when exposed to a field strength of 1-2 V/m. This confirms the suitability of the approach for a wearable device.
- The output of the test board exhibited a considerably higher polarization dependence than expected. This effect is likely due to the size and shape of the ground plane. The unequal size in horizontal and vertical dimensions lead to different probe capacitance depending on which axis the E-field is aligned to. For a polarization insensitive field probe the arrangement of the field probes in a multi-detector setup must therefore be completely symmetrical with respect to the ground plane.
- The output signal of a single diode can be improved by using two diodes per field probe arranged in a so-called voltage doubler configuration as shown in the schematic in Figure 5.

Fields at Work GmbH, Hegibachstrasse 41, 8032 Zürich, Schweiz
Tel. +41 (44) 382 38 31
info@fieldsatwork.ch
www.fieldsatwork.ch

2.3.3 3D field probe detector module

Based on the conclusions and measurement results from the field probe test (paragraph 2.3.1) the next design iteration resulted in the device shown in Figure 7. The design consists of a symmetric circular arrangement of three field probes sharing a common reference plane.

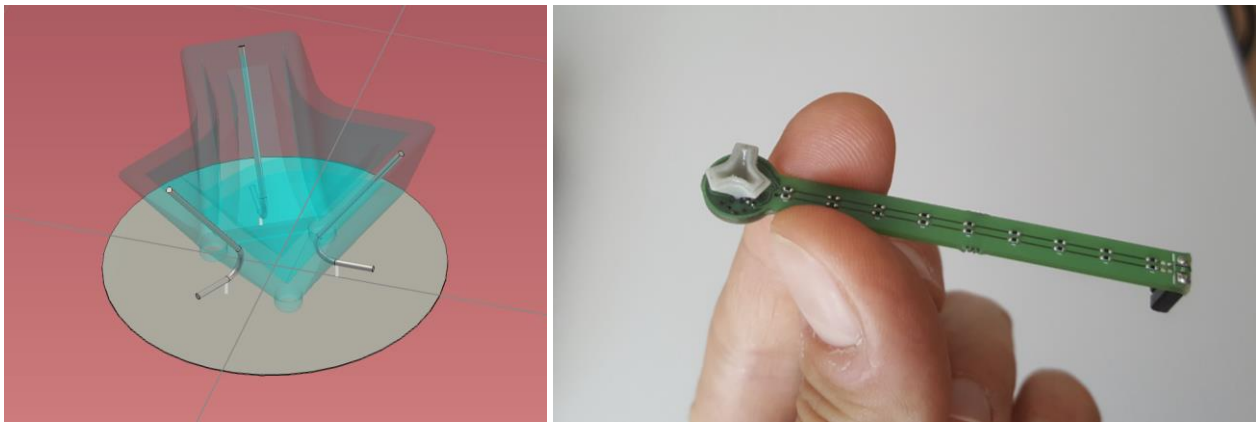

Figure 7: Detector module with a 3-dimensional orthogonal field probe arrangement. CAD drawing of the support and field probe wires (left) and manufactured evaluation prototype on a standard circuit board (right).

The three probe elements are made of thin copper wires. To make sure that these thin elements remain in shape and in the correct place, a 3D printed support was designed into which the wires can be inserted. The support is firmly attached to the circuit board by means of an acrylic adhesive.

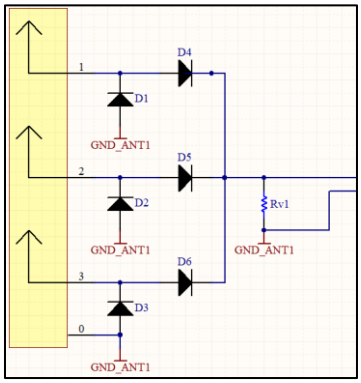

Figure 8: electrical schematic of the 3D field probe module. The three detector axes are combined into a single output.

The outputs of the three detectors are combined into a single output voltage, yielding an omnidirectional probe. The detector module and the output connector are separated form each other by a short section of high resistance transmissin line (see paragraph 2.2.2). Two versions were built with different length of the transmission line (60 mm and 110 mm).

2.3.4 3D field probe evaluation with base station emulator

The 3D field probe detector was evaluated using a GSM/DCS base station emulator (BSE) and a compatible smartphone. A connection is established between the base station emulator and the phone, and a voice call is started. During the voice call it is possible to adjust the transmission power level of the connected phone. Using this setup, it is therefore possible to use a smartphone as RF source with constant RF output

power. The goal of this measurement setup was to evaluate the isotropy of the field probe and to visualize the field strength distribution on the surface of the phone at a distance of 1 cm and 2 cm from the surface. Plastic foam spacers were used to ensure a constant distance for all measurements (Figure 9).

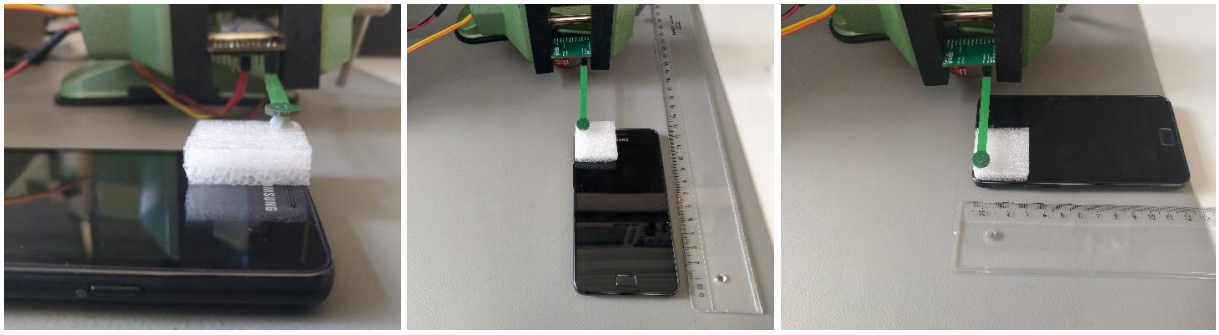

Figure 9: Evaluation of the 3D field probe using a smartphone connected to a base station emulator. The smartphone is performing a voice call and is set to constant output power level (GSM/DCS PCL setting).

The isotropy was measured to be better than ±1.5 dB and ±2.4 dB for the 900 MHz and 1800 MHz band, respectively. The following figure (Figure 10) shows the measurement results of the field strength distribution when transmitting in the GSM 900 band (emulator setting: channel 30, 896.1 MHz). The measurement was carried out at two transmission power settings, referred to as Power Control Level (PCL) in the GSM standard. For the phone model under test, PCL0 corresponds to the maximum transmit power of 33 dBm (2 Watts) whereas PCL6 is a nominal 31 dBm (1.26 Watts) according to the GSM specification. The results are given in Millivolts which is the raw output signal of the used detector. The output voltage is proportional to the RMS power, i.e., the square of the field strength amplitude.

Several observations can be made from the measurement results: There is an obvious “hotspot” in the lower part of the phone, revealing where the antenna for the 900 MHz band is located. GSM 900 is the cellular technology with the highest peak output power in standard mobile handsets. For this reason, the corresponding antenna is often located in the bottom part of the handset to maximize the distance to the head when it is held onto the ear for calling.

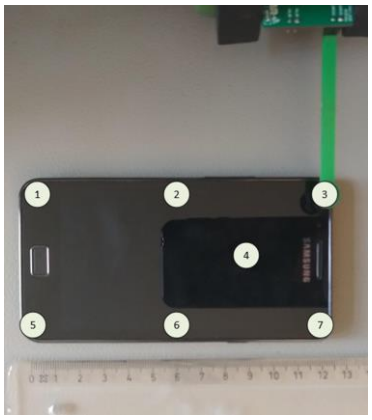

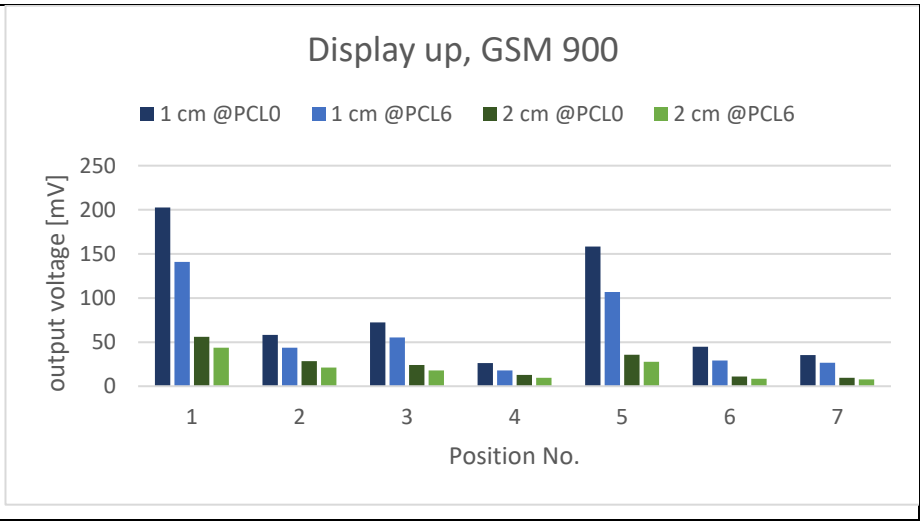

Fields at Work GmbH, Hegibachstrasse 41, 8032 Zürich, Schweiz
Tel. +41 (44) 382 38 31
info@fieldsatwork.ch
www.fieldsatwork.ch

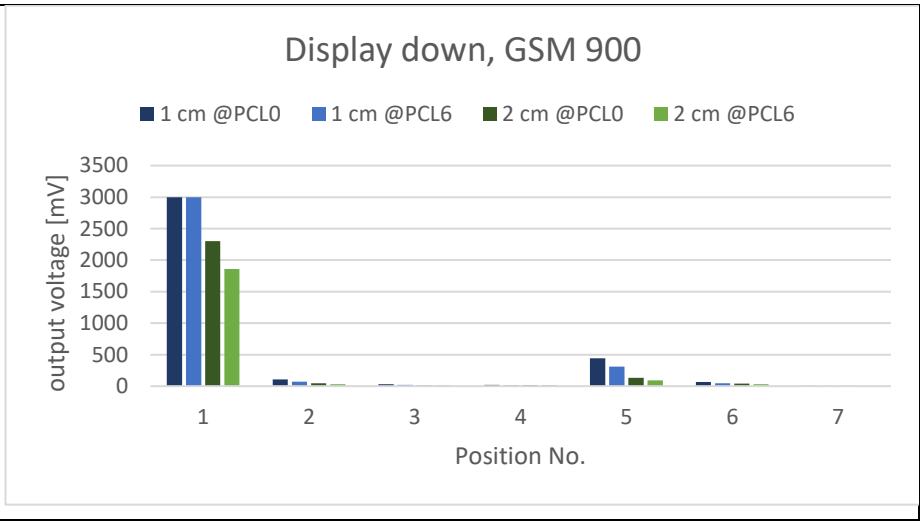

Figure 10: Assessment of the field strength distribution around the smartphone. Measurement locations and raw output values for the assessment of the. Left: display facing up; right: display facing down.

The measurements also reveal that the antenna is most likely mounted on the back side of the phone. This seems to be a very effective measure to shield the strongest fields from the user as the measured values on the "screen side" of the phone are more than 10 times lower than on the side facing away from the user. The field strength directly above the hotspot is strong enough to saturate the field probe at its maximum output voltage of 3000 mV. Except for this case, the relative change of the output signal reflects the expected change in RF output power when switching from PCL0 to PCL6.

Fields at Work GmbH, Hegibachstrasse 41, 8032 Zürich, Schweiz
Tel. +41 (44) 382 38 31
info@fieldsatwork.ch
www.fieldsatwork.ch

2.3.5 Flexible patch “Around the ear” design

The successful evaluation of the 3D field probe, the detector module was integrated into a flexible circuit board shaped in such a way to be placed around the ear of the test subject (Figure 11). This design arrangement includes two 3D field probes with associated high resistance lines, leading to a pre-amplification stage and analog to digital converter in the central part of the circuit board. The straight wide straight strip is a digital interface connecting to the data logger module.

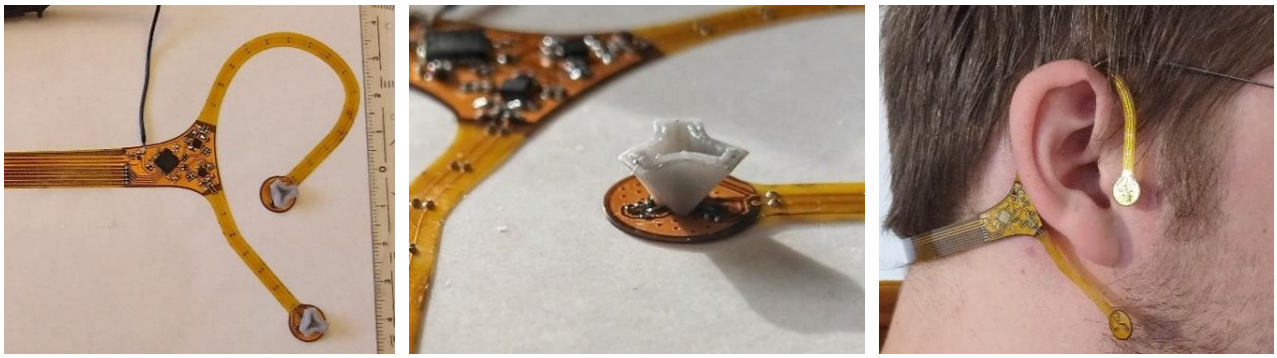

Figure 11: Implementation of the planar device for use at the head around the ear. Left: fully assembled sensor flex print PCB; Middle: close-up of one of the RF detector elements and the readout electronics in the background; Right: sensor worn by a test person. The round ends of the flex PCB represent the location of the detector modules (electronics not mounted in this picture)

2.3.6 Test with smartphone and forced activity

A simple qualitative measurement was set up in the lab to verify the functionality of the “Around the ear” sensor patch: the fully assembled sensor patch was used to detect the emissions of a smartphone actively transferring data triggered by a data transfer speed benchmarking app (cnlab UX Test by cnlab AG). The phone was connected to the internet via cellular network and was placed at about 15 mm from the surface of the sensor patch (Figure 12).

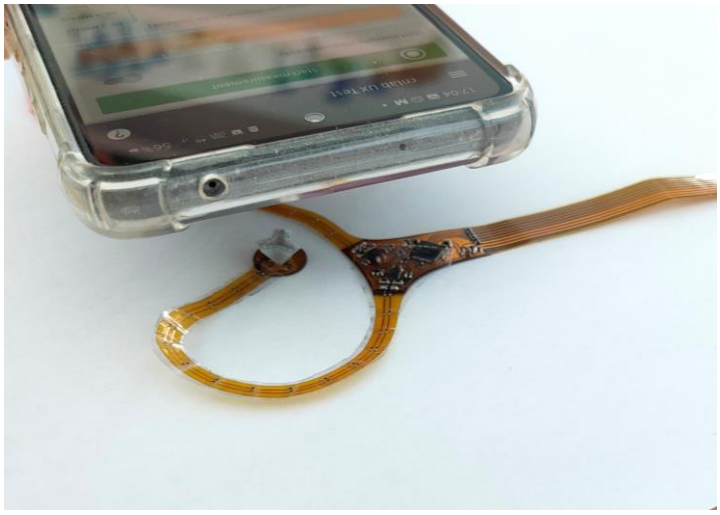

Figure 12: Measurement setup for the first functional test

Figure 13 shows the raw measurement data from one of the two detectors after four speed test runs using WiFi and cellular data. Each run of the speed benchmark performed by the app consists of following three

measurements: 1) latency, 2) download speed and 3) upload speed, which are performed in this sequence. The resulting pattern is consistent but shows some variability from run to run, even though the experiment was performed in a static environment. As expected, the upload test results in the highest measured EMF emissions, followed by the download test and the latency test, which produces a less predictable and sometimes "spiky" uplink activity.

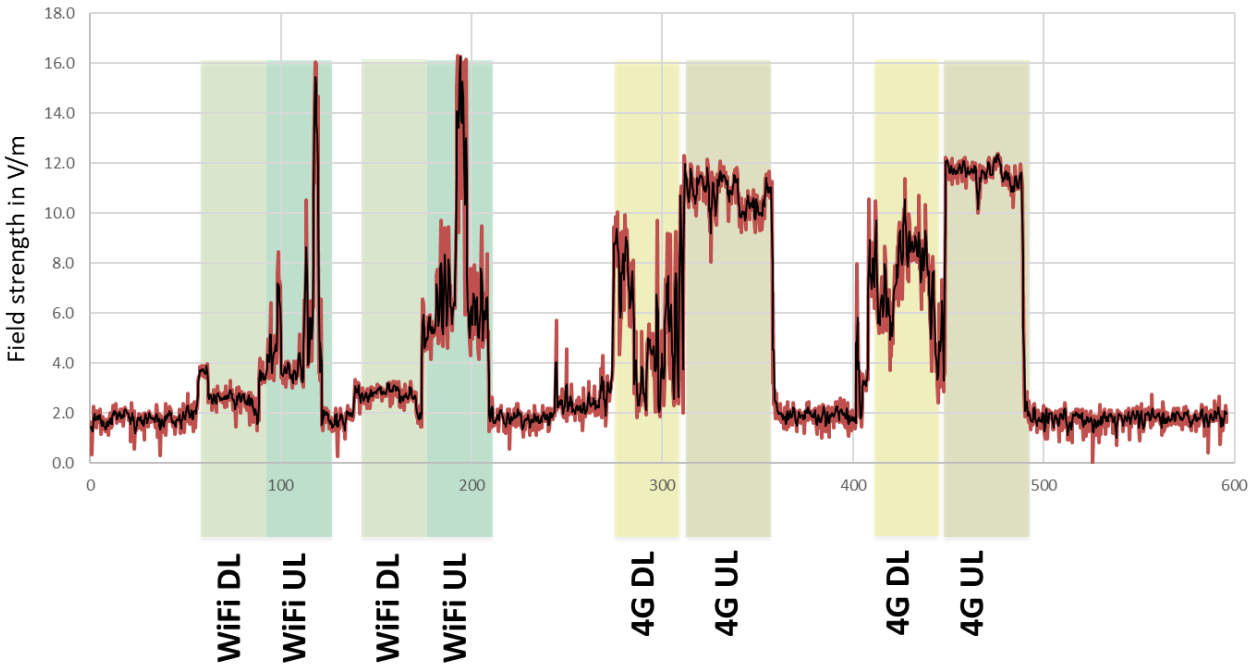

Figure 13: Laboratory assessment of the "around the ear" sensor performance while performing four runs (2x using Wi-Fi and 2x using cellular data) with a speed test app (cnlab UX Test).

2.3.7 Test outcome and conclusions

The development iterations and design steps so far demonstrated the feasibility of the approach, its adequate performance, and its added value for evaluating the field strength close to EMF emitting devices in use. At this stage the design was therefore in principle ready to be finalized into a final prototype for a small series production run.

However, additional practical tests and experiments of the functional prototypes revealed several practical shortcomings of the design which would have been a risk for the outcome of a study involving several uninformed participants. A detailed summary of the identified issues and consequences is given in section 2.4.

Fields at Work GmbH, Hegibachstrasse 41, 8032 Zürich, Schweiz
Tel. +41 (44) 382 38 31
info@fieldsatwork.ch
www.fieldsatwork.ch

2.4 Redefining the design

Despite the successful tests of the concept and design prototypes, we decided to perform major refinement to the design of the field probe. This section gives a detailed overview of the factors that lead to this additional iteration, the identified issues and how these were addressed.

2.4.1 Technical challenges

Sensitivity: The lower the detection limit of a measurement device, the more usable measurements can be obtained in a measurement campaign. As it can be seen in Figure 13, the lower detection limit (visible as noise floor) of the “around the ear” sensor design is about 2 V/m. This is a reasonable value as the expected field strength in the near field can reach several times this value. However, achieving a lover detection limit would strongly improve the versatility of the device and lower the amount of “non-detects” in a measurement campaign. In addition, a low sensitivity requires higher signal amplification which in turn accentuates the undesired influences of thermal drift and component and manufacturing tolerances.

Temperature drift: Diode detectors are intrinsically prone to some degree of temperature drift as the threshold voltage of a PN junction is a function of temperature. This effect leads to variations in the measured output voltage of the field probe which are not related to the E-Field strength. This makes it difficult to perform a stable calibration of the field probe at low field strength levels. During our tests we observed pronounced transients of the output signal when the path was moved to different environments or subjected to thermal transients. In some cases, the thermal drift caused a change in the output signal equivalent to an EMF irradiation of 10 V/m or more. Although it is possible to discern thermally induced drift from EMF activity to some extent based on the variation of the signal over time, the magnitude of the effect was determined to be too pronounced to guarantee good measurement results over a wide range of ambient conditions (indoor and outdoor scenarios at different times of the year). We therefore decided to update the design with an analog temperature compensation. This involves the addition of a reference diode, whose output is subtracted from the detector signal. However, this approach requires the diodes to be used in a biased configuration, adding complexity to the detector design.

2.4.2 Manufacturing and complexity of design

The added complexity of the detector with temperature compensation made it impossible to fit the 3D configuration into the same restricted volume using affordable standard manufacturing techniques. The electrical design of the detector had therefore to be simplified. Numerical simulations showed that the electric field close to the skin/air interface are expected to be mostly perpendicular to the skin surface due to the high conductivity of the skin (Figure 14). We decided to exploit this fact to reduce the complexity of the field probe. The 3D arrangement was therefore replaced by a single detector oriented perpendicularly to the skin. In our opinion the benefit of a temperature compensated detector outweighs the loss in accuracy due to the lower number of detectors. This step allowed also to simplify the manufacturing process and reduce the number possible points of failure. The single detector arrangement allows for a probe shape with higher capacitance (and thus better sensitivity) and does not rely of the small 3D printed part which was found to be prone to get caught in clothing and cause damage to the detector in the process.

Fields at Work GmbH, Hegibachstrasse 41, 8032 Zürich, Schweiz
Tel. +41 (44) 382 38 31
info@fieldsatwork.ch
www.fieldsatwork.ch

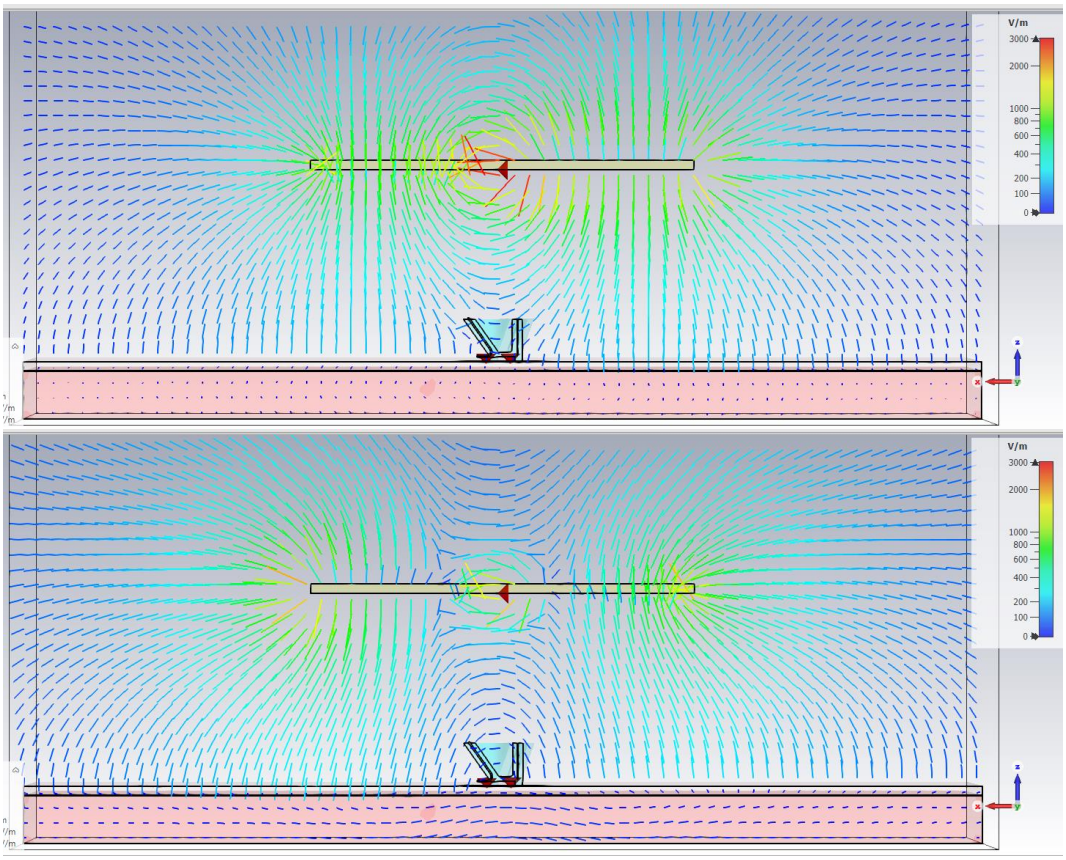

Figure 14: Simulation of the E-field distribution of a small dipole antenna placed at 20 mm from a layered skin model. Due to the high conductivity of the skin, the electrical field lines at the skin/air interface are mostly oriented perpendicular to the skin surface. E-field at 800 MHz (top) and 2.5 GHz (bottom).

Mechanical stability of the assembly: After some usage we noticed that the measurements of some prototypes started to exhibit an intermittent erroneous behavior. This could be eventually traced down to microscopic cracks forming in the flexible conductors of the high resistance lines over time. This issue is not completely solved yet. Possible approaches to tackle this issue are a different choice of materials, modifications of the circuit board stackup and its geometry to limit the bending radius, for example by embedding it into a plaster tissue. The currently adopted workaround consists in stiffening the patch to prevent excessive bending to be applied to the device.

2.4.3 Usage and handling

The “around the ear” device turned out to be quite cumbersome to apply to the skin in practice. The complex shape requires several attachment points and is very challenging to mount or reattach without the help of a second person. Furthermore, its shape is tailored to be used in a very specific location. Measurements on other parts of the body would require different specific shapes and designs. We therefore decided to modify the patch geometry in such a way to be applicable more universally in different locations of the body (see section 4.2.1).

2.4.4 Additional unexpected hurdles leading to delays

The additional iteration caused a considerable delay in the planned development schedule of the field probe. This delay was aggravated by component shortage, which affected crucial elements of our original design, and forced us to look for alternative parts and reiterate part of the initial evaluation process. In

Fields at Work GmbH, Hegibachstrasse 41, 8032 Zürich, Schweiz
Tel. +41 (44) 382 38 31
info@fieldsatwork.ch
www.fieldsatwork.ch

addition, delivery and shipping times of printed circuit boards and other custom-made parts were significantly longer during COVID pandemic due to worldwide lockdowns and associated disruptions of the manufacturing supply chains.

Fields at Work GmbH, Hegibachstrasse 41, 8032 Zürich, Schweiz
Tel. +41 (44) 382 38 31
info@fieldsatwork.ch
www.fieldsatwork.ch

3 Device Calibration

3.1 General considerations

Calibration is a crucial part of every measurement device. The calibration process allows to relate and scale the raw output values of the measurement device to meaningful units. In case of a field probe, the output value shall be expressed in V/m. To create the corresponding calibration table, a measurement setup is required which allows to create a reproducible environment with well-defined field strength values of different amplitudes. For optimum accuracy, the calibration environment should replicate as accurately as possible the environment in which the device to be calibrated is operated in its intended use. Latter requirement is not trivial to fulfil for a near field probe.

3.2 Characterization in TEM-Cell

3.2.1 Principle, Advantages and Limitations

A TEM cell is a transmission line section which is accessible from the sides. The field strength between the plates of the structure is homogeneous, well defined, and proportional to the RF power applied to the TEM cell. The second port of the cell is terminated with the characteristic impedance of the transmission line. A power meter can be connected to the output port to monitor the power for additional confidence. Ideally, all RF power applied to the TEM cell exits from the output port. In a real setup, some power is lost in impedance mismatch (reflection), leakage radiation, and resistive losses along the transmission line.

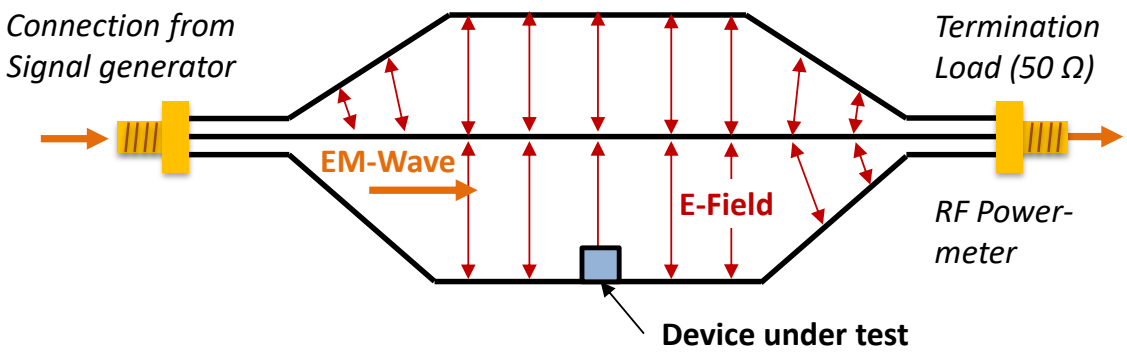

Figure 15: Working principle and E-field distribution of a TEM Cell

The main advantage of a TEM cell is its well-defined and reproducible EM Field distribution. There is a direct relationship between the input power and the electrical field strength between the plates. However, the field in a TEM cell approximates a far field situation as the relationship between E-field and H-field is 377 Ohms like in free space at the DUT location. It is therefore not possible to reproduce an electrical near field with this setup.

The initial calibration of all manufactured field probes was performed in a TEM cell. The setup is shown in Figure 16. Although its field distribution may not represent an ideal representation of a near field exposure, the high reproducibility of this approach is highly valuable during the development process to assess variability, drift and other parameters that may change over time.

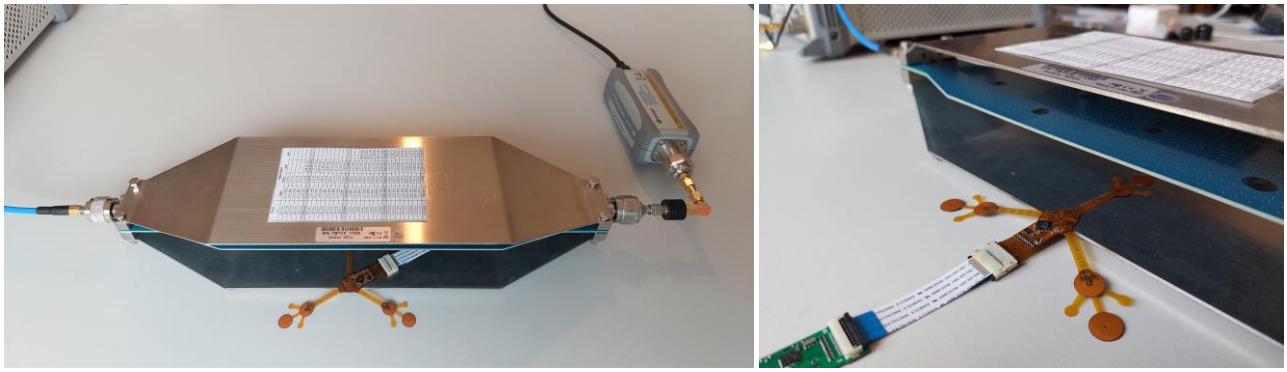

Figure 16: TEM Cell setup used for the initial calibration of the field probes.

3.3 Characterization in the near field

The most realistic calibration environment for the presented field probe would be an exposure in the near field of an actual smartphone antenna. This approach cannot be directly implemented in practice because it relies on several factors that are either not known or cannot be readily controlled, such as the exact geometry of the antenna and the exact output power of the phone to calculate the reference E-field distribution used to calibrate the device.

It is however possible to conceive a controlled measurement setup which approximates such a near field exposure. In the following two possible approaches are presented and discussed.

3.3.1 Advantages and limitations

Well-defined and reproducible near field distributions can be created using simple antenna geometries which are relatively easy to characterize numerically. The numerical characterization is necessary to know the field strength at a specific location and distance from the antenna geometry for any given input power.

The main challenge of this approach is the fact that near fields are intrinsically inhomogeneous and exhibit strong location dependent gradients. The near field region of an antenna extends to about one half of a wavelength around the antenna at the excitation frequency. The positioning of the device under test gets therefore increasingly challenging at higher frequencies (the free-space wavelength at 6 GHz is 5 cm). Furthermore, it is not trivial to define the exact reference amplitude of the applied field strength as the field strength is likely not to be homogeneous within volume of the field probe.

3.3.2 Possible setups

Following setups have been considered for a near field characterisation of the device:

Dipole antenna: An electrically small (i.e. short in terms of wavelength) dipole antenna has well-defined electrical field distribution and can be modelled both numerically and analytically to compute the field strength distribution for a given input power. This setup can be quite broadband as there is no fundamental lower frequency limit to achieve the same electrical field distribution. There is an upper frequency limit though, which is given by the size of the dipole. The structure must be “electrically small” for all frequencies of operation. A practical challenge consists in feeding the Dipole antenna. RF signal generators are equipped with coaxial outputs (i.e., single-ended) whereas a dipole expects a balanced / differential feed. A balun is required for the conversion between the two modes of signal propagation. This conversion

introduces additional complexity and uncertainties as accurate broadband baluns are very difficult to manufacture and model at microwave frequencies.

Waveguide with iris: The rectangular waveguides and the associated propagation modes are also a predictable and suitable for modelling. Coaxial to waveguide transitions are well defined standard components. The electromagnetic field in a rectangular waveguide has a higher impedance than free space, meaning that the E to H ratio is higher. By introducing irises, i.e., metallic obstructions and openings of different sizes in the cross section of the waveguide, the ratio of the E- and H-field in the opening can be modified in a predictable manner (Figure 17). The field probe could therefore be calibrated by placing it into the iris. The main disadvantage of a waveguide approach is its narrow bandwidth. The usable frequency range of a waveguide is less than one octave. For a calibration over the full measurement range of the device several waveguides of different sizes would therefore be required.

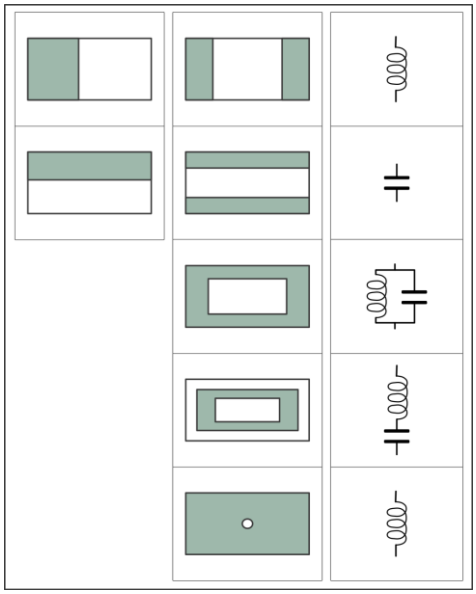

Figure 17: Waveguide irises and their equivalent circuit elements (source: Wikipedia).

Fields at Work GmbH, Hegibachstrasse 41, 8032 Zürich, Schweiz
Tel. +41 (44) 382 38 31
info@fieldsatwork.ch
www.fieldsatwork.ch

4 Implementation

4.1 Overview

Figure 18 shows a block diagram of all components of the implemented measurement system. The system consists of two wearable parts (sensor patch and data logger unit) and a docking station. The docking station serves two purposes. It is used to charge the battery of the data logger unit and provides a mean to connect the data logger unit to a PC to access the measurement data.

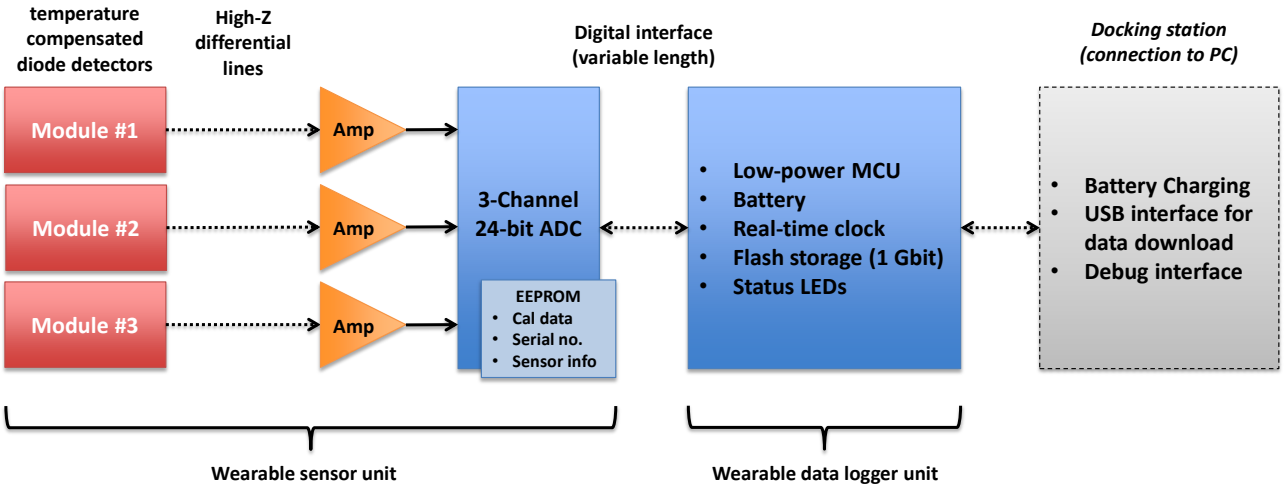

Figure 18: System block diagram of the final implementation.

The wearable part of the system has been deliberately divided into two parts. The sensor unit (patch) is the part designed to be attached directly to the skin. Its design is therefore optimized for minimum size and weight. The sensor unit contains the sensor elements and the associated analog signal conditioning electronics. To prevent signal degradation, the analog to digital converter is also part of the sensor patch assembly. This allows the sensor patch to be connected to the data logger unit by means of a purely digital interface which is not affected by noise and interference. Each sensor patch also contains a section of non-volatile memory (EEPROM) to store the calibration data and other auxiliary information.

Data acquisition, storage, and the power supply is provided by the data logger unit. The data logger unit is powered by a small rechargeable battery. This prevents it to be as thin and lightweight as the sensor patch, but it is still of very moderate size such that it can easily be worn on the body (see Figure 19).

4.2 System components

4.2.1 Sensor patch assembly

Each sensor patch includes 3 cylindrical E-Field sensors elements referred to as channel A, B and C. The sensor is connected to the logger module via the digital sensor interface. An interface extension cable can be used to increase the distance between patch and logger if required.

Two little protrusions on the side of each sensor element can be used to attach the patch to the skin of the test person using e.g., medical tape.

Fields at Work GmbH, Hegibachstrasse 41, 8032 Zürich, Schweiz
Tel. +41 (44) 382 38 31
info@fieldsatwork.ch
www.fieldsatwork.ch

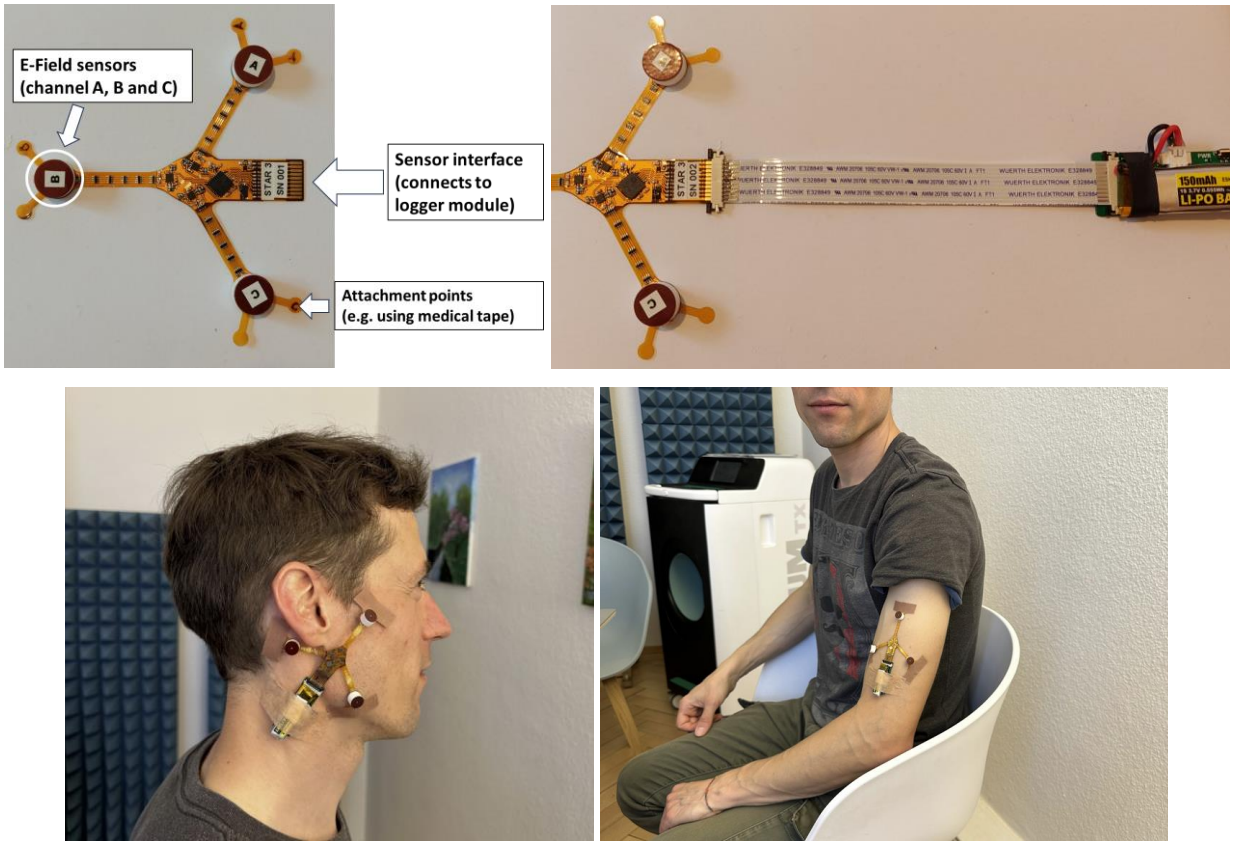

Figure 19: top left: wearable sensor path assembly (3-sensor STAR arrangement); top right: sensor unit attached to the data logger unit with extension cable. Bottom: possible application methods.

4.2.2 Data Logger Unit

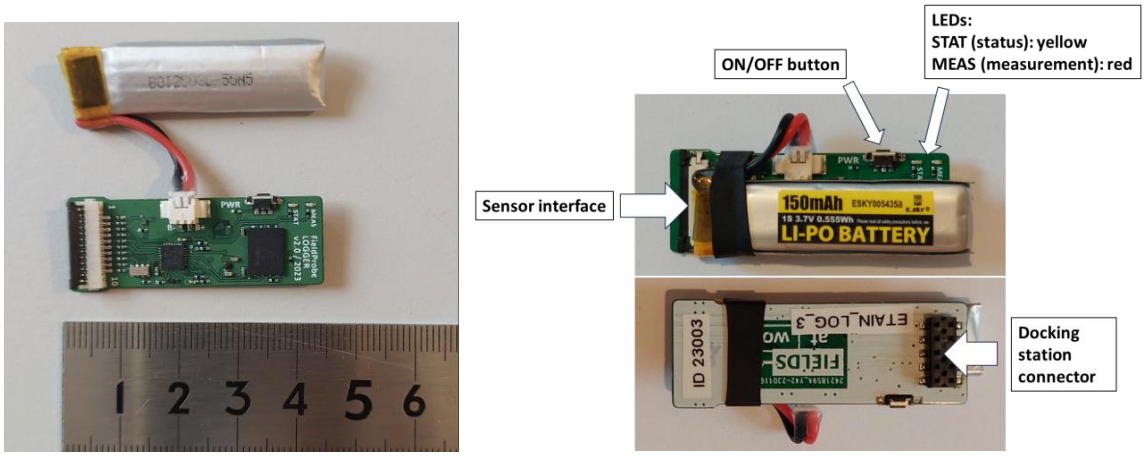

Figure 20: Logger module: Dimensions (left) and user elements on the top and bottom of the module (right)

4.2.3 Docking station

The docking station is required to download the data from the logger module and for recharging its battery. The correct position of the logger is outlined in white on the silkscreen of the PCB.

Fields at Work GmbH, Hegibachstrasse 41, 8032 Zürich, Schweiz
Tel. +41 (44) 382 38 31
info@fieldsatwork.ch
www.fieldsatwork.ch

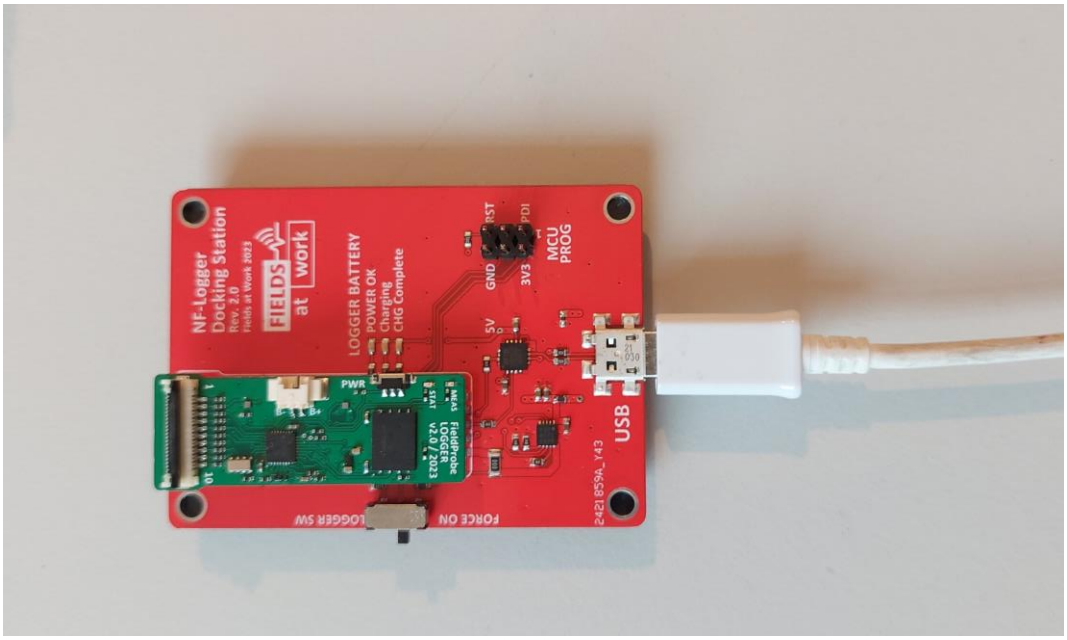

Figure 21: USB docking station (shown with attached logger module)

4.2.4 Software and user interface

The data on the device is accessed through a Windows application when the data logger is connected to the PC via the docking station.

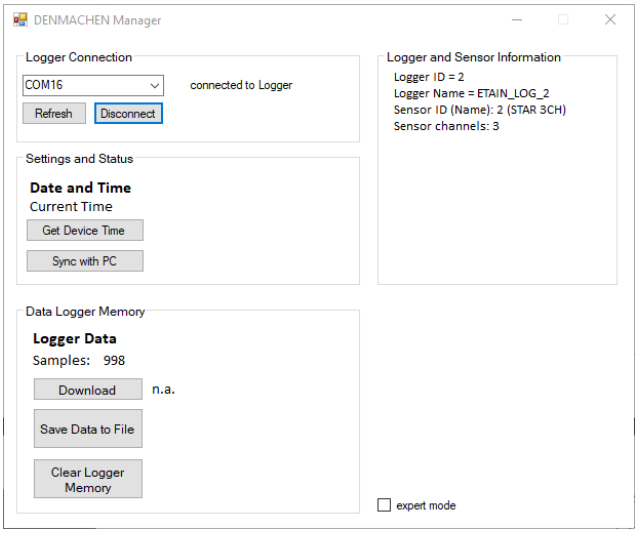

Figure 4: Main window of the PC application for connecting and downloading the measurement data from the patch

4.3 Calibration and characterization of the "final prototypes"

4.3.1 Overview

The characterization and calibration of the final design prototypes is carried out in a small TEM cell (TekBox Model TBTC0) specified up to 6 GHz. The small size of this model allows to achieve the necessary high field strength values without the need of excessive RF input power. Less than 200 mW are required to obtain an electric field strength of 100 V/m in the TEM cell.

A first characterization is performed at several frequencies within the measurement range of the near field probe. For each frequency, a mapping between applied field strength levels and sensor output is made. Ideally, this mapping is independent from the frequency of the electromagnetic field. However, some frequency dependence cannot be avoided. The baseline amplitude response calibration of the sensor is determined at a frequency of 250 MHz. This relatively low frequency ensures that the field distribution in the TEM cell is very well defined. Previously performed tests have also shown that the response of the probes at 250 MHz represent the overall response very well (Figure 22). The calibration values are stored in the non-volatile memory of the patch.

4.3.2 Frequency response

Figure 22 shows the typical relative frequency response of one of the sensors channels. The measurement is performed at several frequencies within the measurement range of the near field probe. The raw sensor output at 1 GHz is taken as a reference and compared to the response at other excitation frequencies at the same RMS field strength value. Ideally, the sensor response is independent from the frequency of the electromagnetic field. However, some frequency dependence cannot be avoided due to various parasitic and non-ideal properties of the components, sensor geometry and the measurement setup. The sensors feature a very flat frequency response from 100 MHz to 5 GHz except for a moderate overshoot around 3.5 GHz. The exact cause for latter phenomenon could not be determined. It might be related to mild resonance effects within the electronic components of the detector. This largely flat frequency response avoids the need for a frequency specific calibration for most purposes.

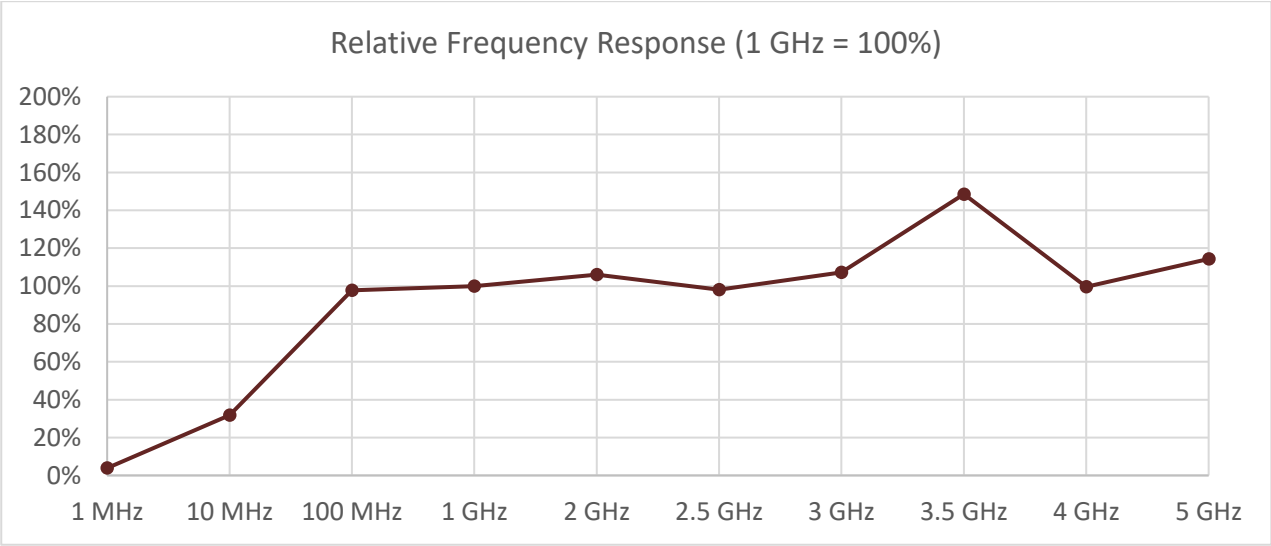

Figure 22: Relative frequency response of the final implementation

4.3.3 Sensitivity and Dynamic Range

The plot in Figure 23 shows the calibration curve of the three channels of one of the sensor patches obtained with the calibration in the TEM cell. The response of the sensors corresponds to the expected behavior of a diode-based detector. Up to about 25 V/m the curve follows a quadratic relationship between applied field strength and output signal and transitions to a linear dependence at higher field strengths.

Fields at Work GmbH, Hegibachstrasse 41, 8032 Zürich, Schweiz
Tel. +41 (44) 382 38 31
info@fieldsatwork.ch
www.fieldsatwork.ch

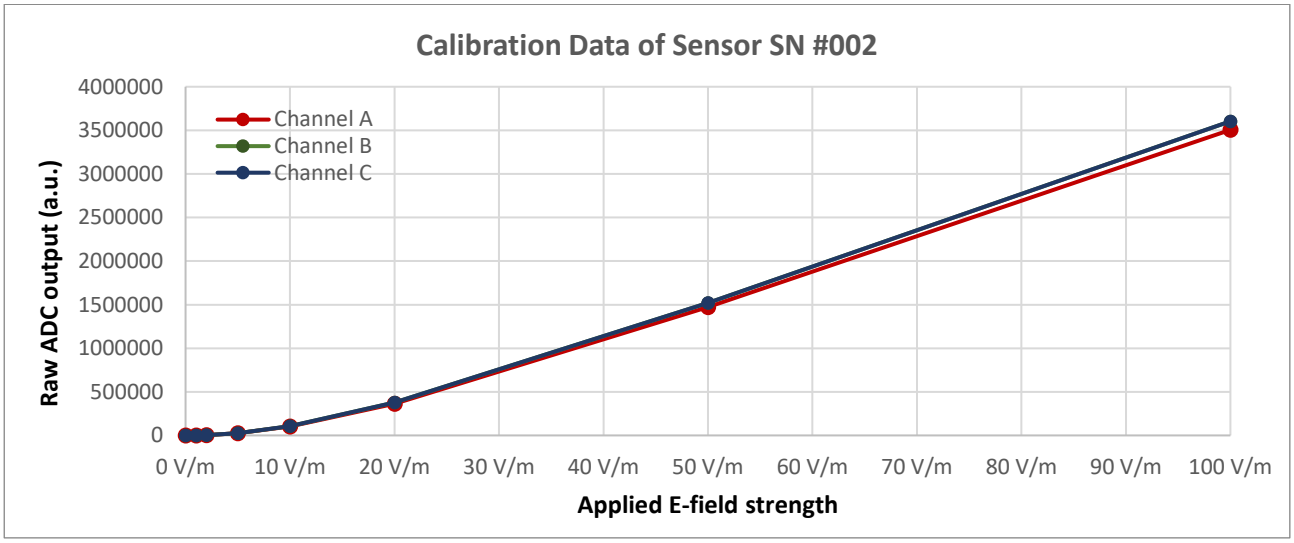

Figure 23: example of a calibration curve. The tree channels of the probe show a very similar response.

Based on the calibration curve (as the example shown in Figure 23) and the saturation output voltage of the probe it is possible to estimate the maximum detectable field strength. The following table (Table 2) shows the corresponding values for the tree first STAR prototypes.

Sensor No.	Design	Channel A	Channel B	Channel C
SN 001	"Star 3-channel"	267 V/m	139 V/m	258 V/m
SN 002	"Star 3-channel"	221 V/m	212 V/m	217 V/m
SN 003	"Star 3-channel"	225 V/m	227 V/m	243 V/m

Table 2: Maximum detectable field strength (saturation limit) of the three manufactured sensor units (extrapolated from 100 V/m calibration point)

The minimum detectable field strength under stable laboratory conditions is about 0.5 V/m (three sigma of the measurement noise). If uncertainties due to residual temperature drift are included, this value increases to about 2 V/m. This yields a dynamic range of over 35 dB even in the worst case (2 V/m to 139 V/m).

Fields at Work GmbH, Hegibachstrasse 41, 8032 Zürich, Schweiz
Tel. +41 (44) 382 38 31
info@fieldsatwork.ch
www.fieldsatwork.ch

5 Measurement campaign

A measurement campaign is currently taking place within the ETAIN project in which multiple near field probes (mounted on the ear, on the abdomen and on the chest of the test person) are used in parallel with an ExpoM-RF 4 exposimeter (Sandoval-Diez et al, 2023). Several phone usage scenarios are performed forcing downlink and uplink activity (voice call, video call, streaming, etc.) and using different wireless technologies (4G, 5G, Wi-Fi). As this campaign is still in progress, the results are preliminary and confidential.

Fields at Work GmbH, Hegibachstrasse 41, 8032 Zürich, Schweiz
Tel. +41 (44) 382 38 31
info@fieldsatwork.ch
www.fieldsatwork.ch

6 Conclusions and Outlook

6.1 Discussion of current concept and implementation

The results of this research project demonstrated the feasibility of an on-body field probe, although the effort required for the realization of a functional prototype have been higher than anticipated. The availability of a low-power wearable EMF measurement device opens new possibilities and study designs for epidemiological research. The current design of the system is suitable to be used in research studies with informed people and will contribute to close knowledge gaps regarding time patterns and distribution of near field exposure in real world scenarios. The findings of this project serve as a basis for the measurement campaign performed within the ETAIN European project. The presented measurement approach has gained attention in the bioelectromagnetics community and there are plans for other measurement campaigns using the on-body field probe.

6.2 Outlook

The current implementation of the measurement system is modular. The measurement patch and the data logger can be separated. The interface between the two parts includes a versatile digital serial bus and a power supply line. This gives full flexibility for the creation of differently shaped sensor patches and sensor arrangements, and even to include completely different measurement principles and additional sensors with digital interface (accelerometer, temperature etc.) adapted to a wide range of study protocols.

The current design has still to be optimized for series production to be suitable for large-scale studies with dozens or even hundreds of participants. In the current state of development, the manufacturing process is lengthy and involves several manual steps, leading to high costs per device. In this context it is also necessary to improve the mechanical stability of the wearable device to ensure reliable measurement results under varying environment conditions with no need for the participants to worry about the presence of the device, for example by integrating all electronics into a single sealed adhesive patch.

Fields at Work GmbH, Hegibachstrasse 41, 8032 Zürich, Schweiz
Tel. +41 (44) 382 38 31
info@fieldsatwork.ch
www.fieldsatwork.ch

7 Financial Summary

7.1 Financial Summary

Description	FaW invoice No.	Revenues	Other costs	Salay costs	Total Expenses
Tranche 1 FSM	FW-20191102-1	30’000			
2019			200	2’000	2’200
Tranche 2 FSM	FW-20200305-1	30’000			
2020			600	16’000	16’600
2021			1’300	20’000	21’300
Tranche 3 FSM	FW-20220103-1	67'500			
2022			7'500	50'000	57'500
2023			6'400	46'000	52'400
Schlusstranche FSM		22'500			
Total		**150’000**	**16’000**	**134’000**	**150’000**

Table 3: Financial summary. All values are in CHF.

Fields at Work GmbH, Hegibachstrasse 41, 8032 Zürich, Schweiz
Tel. +41 (44) 382 38 31
info@fieldsatwork.ch
www.fieldsatwork.ch

8 References

- Nekane Sandoval-Diez, Alberto Castro, Timon Schmid, Marco Zahner, Arno Thielens, Jürg Fröhlich, Anke Huss, and Martin Röösli, Derivation of Calibration Functions for an Open-Access Smartphone App for RF-EMF Exposure Assessment - Measurement Protocol, BioEM 2023, Oxford, GB.
- Marco Zahner, Fabian Scheider, Martin Röösli, Jürg Fröhlich, A near field measurement approach for comprehensive on-body uplink/downlink exposure measurement, BioEM 2022, Nagoya, JP.
- Marco Zahner, Schliessen einer Lücke: Messen von Nahfeldern direkt am Körper, FSM Science Brunch 35 - Herausforderungen bei der Erfassung der Exposition gegenüber EMF, 2023, Zurich, Switzerland

Fields at Work GmbH, Hegibachstrasse 41, 8032 Zürich, Schweiz
Tel. +41 (44) 382 38 31
info@fieldsatwork.ch
www.fieldsatwork.ch

9 Appendix: Manual / Quick guide

9.1 Hardware Components and User Elements

9.1.1 Logger module

The following picture shows an overview of the user elements of the logger module:

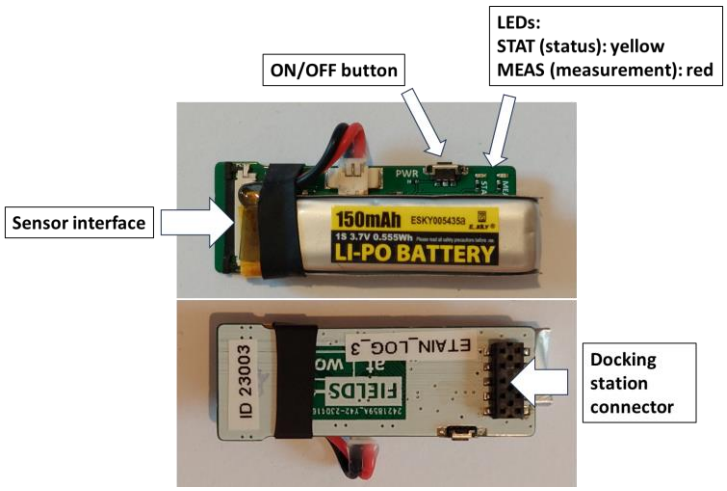

Figure 24: User elements of the logger module

9.1.2 Logger module: status LEDs

Status / operational mode	STAT LED (yellow)	MEAS LED (red)
Normal measurement mode	(OFF)	flashing (interval 500 ms)
Power down procedure (takes about 5 seconds)	flashing (interval ca. 500 ms)	(OFF)
Connection mode (connected to PC)	Continuously on	(OFF)
Initialization error (e.g., no sensor connected)	Quickly flashing (100 ms)	Quickly flashing (100 ms)

Table 4: Status LEDs of the logger module

Fields at Work GmbH, Hegibachstrasse 41, 8032 Zürich, Schweiz
Tel. +41 (44) 382 38 31
info@fieldsatwork.ch
www.fieldsatwork.ch

9.1.3 Docking station

The following picture shows an overview of the user elements of the docking station:

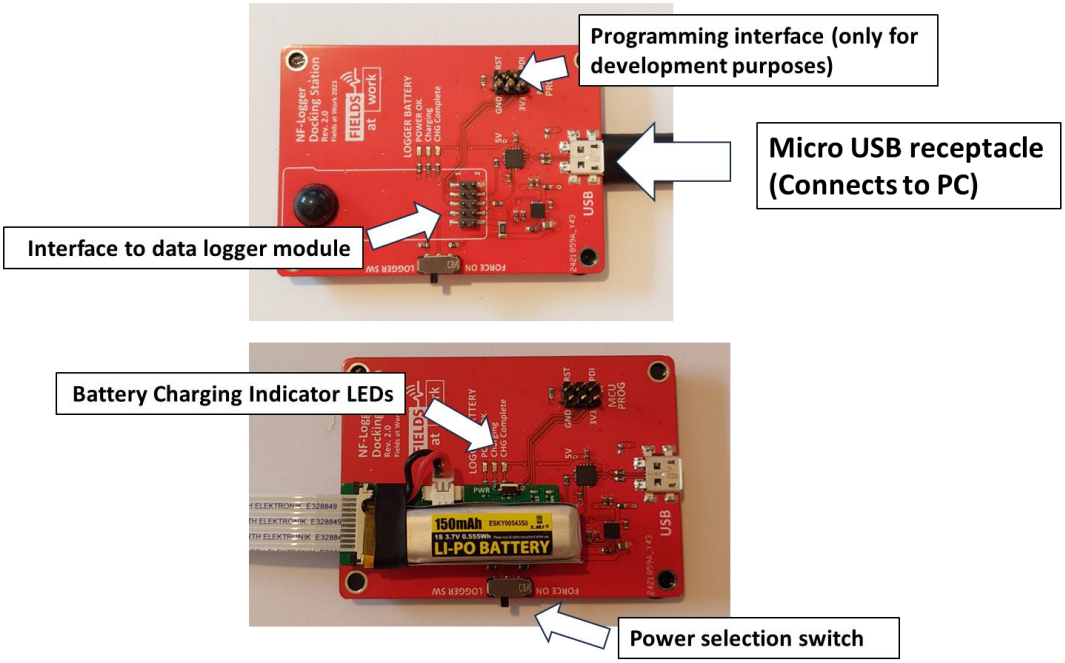

Figure 25: User elements of the docking station

9.1.4 Docking station: indicator LEDs

The docking station is provided with three indicator LEDs for user feedback. These LEDs mainly relate to power management.

- "POWER OK" (red): Indicates whether power is provided by the USB bus
- "Charging" (red): Battery charging in progress (only valid with attached logger module)
- "CHG complete" (green): battery is fully charged (only valid with attached logger module)

9.1.5 Docking station: power selection switch

The power selection switch changes the behavior when connecting to the PC software:

- If the switch is in "FORCE ON" position, the logger is automatically powered on and put into connection mode as soon as it is plugged onto the docking station. In this mode the logger can only be completely switched off if it is physically disconnected from the docking station.
- In "LOGGER SW" position, the logger behaves normally and must be switched on manually (ON/OFF switch) before a connection to the PC can be established.

9.2 Usage and Handling

The measurement and power management are all managed by the data logger unit. The data logger unit has a minimal user interface consisting of a tiny push button and two status LEDs for visual feedback.

Fields at Work GmbH, Hegibachstrasse 41, 8032 Zürich, Schweiz
Tel. +41 (44) 382 38 31
info@fieldsatwork.ch
www.fieldsatwork.ch

9.2.1 Starting and stopping a measurement

When the data logger unit is in the off state, pressing and holding the ON/OFF button for 1-2 seconds will put the unit into measurement mode. The red MEAS LED starts to flash regularly (once every measurement, i.e., 2 times per second)

The measurement can be stopped any time by pressing and holding again the push button of the logger unit. As soon as the STAT LED starts blinking the ON/OFF button can be released. After 2-3 seconds the device powers down into OFF state.

Every time a measurement started the new data is appended to the already existing data until the logger memory is full (no data is deleted). The logger memory can only be cleared using the PC application.

9.3 Output Data Format

The basic structure of the exported data looks like in the example below. There is a short header with the settings and ID numbers of the components followed by the actual measurement data. The measurement data a timestamp for each measurement and the values for the three channels of the data logger. Unused channels contain zeros or invalid data. The error column is used to signalize special events or errors detected by the software of the logger unit.

	A	B	C	D	E	F	G	H	I
1	Logger ID:	23002							
2	Logger Name:	ETAIN_LOG_2							
3	Sensor ID:	2							
4	Sensor Name:	STAR 3CH							
5	Sensor Channels:	3							
6	Timestamp (yyyy-M	Channel A (V/m)	Channel A (RAW)	Channel B (V/m)	Channel B (RAW)	Channel C (V/m)	Channel C (RAW)	error	
7	13-07-23 08:25	1.94	8359191	0	8521563	0.44	8397897	0	
8	13-07-23 08:25	1.95	8359251	0	8520790	0	8397165	0	
9	13-07-23 08:25	1.95	8359264	0	8520753	0	8397230	0	
10	13-07-23 08:25	2.1	8360079	0	8521528	0.55	8397991	0	
11	13-07-23 08:25	2.11	8360143	0	8521431	0.56	8397994	0	
12	13-07-23 08:25	2.1	8360057	0	8521507	0.57	8398008	0	
13	13-07-23 08:25	1.94	8359215	0	8520807	0.52	8397966	0	
14	13-07-23 08:25	1.93	8359175	0	8521585	0.65	8398083	0	
15	13-07-23 08:25	2.07	8359907	0	8521469	0.61	8398045	0	
16	13-07-23 08:25	1.93	8359152	0	8521555	0.58	8398019	0	
17	13-07-23 08:25	2.06	8359862	0	8521417	0.67	8398112	0	
18	13-07-23 08:25	1.91	8359057	0	8521447	0.6	8398037	0	
19	13-07-23 08:25	2.07	8359912	0	8521461	0.64	8398074	0	
20	13-07-23 08:26	2.86	8365070	0	8522024	1.01	8398567	0	
21	13-07-23 08:26	2.61	8363288	0	8522189	1.05	8398634	0	
22	13-07-23 08:26	2.52	8362650	0	8521193	0.28	8397807	0	
23	13-07-23 08:26	2.55	8362839	0	8522068	1.04	8398622	0	
24	13-07-23 08:26	2.39	8361780	0	8521083	0.09	8397747	0	
25	13-07-23 08:26	2.35	8361518	0	8521323	0.98	8398523	0	
26	13-07-23 08:26	2.42	8362017	0	8521966	0.98	8398533	0	
27	13-07-23 08:26	2.28	8361132	0	8521972	0.99	8398538	0	
28	13-07-23 08:26	2.38	8361737	0	8521891	1.06	8398663	0	
29	13-07-23 08:26	2.24	8360845	0	8521971	1.08	8398701	0	
30	13-07-23 08:26	2.23	8360803	0	8521956	0.94	8398467	0	

Figure 26: Example output data

Fields at Work GmbH, Hegibachstrasse 41, 8032 Zürich, Schweiz
Tel. +41 (44) 382 38 31
info@fieldsatwork.ch
www.fieldsatwork.ch

9.4 System specifications

9.4.1 Sensor

Frequency range	100 MHz to 6.0 GHz nominal
Detection method	Broadband diode detector
Polarization	Main sensitivity to E-Field perpendicular to sensor surface / skin
Dynamic range	Min. 35 dB
Measurement range	*Measurement frequency* — *Typical lower and upper detection limit* 100 – 6 GHz — 1 V/m — 150 V/m
Calibration	Calibration in TEM cell Calibration factors are determined for following frequencies (as necessary) 100, 850, 1800, 2100, 2500, 3600, 5200 MHz

9.4.2 Data Logger

Measurement interval	Default: 0.50 sec (2 measurements / second) on three channels Longer and shorter intervals (down to 4 measurements per second) can be accommodated with customized software. The shortest possible measurement interval might depend on the number of sensors used by the data logger
Timing	Integrated precision real-time clock (3 ppm accuracy)
Battery	150 mAh rechargeable Li-Ion battery (charging via docking station) Expected runtime: > 100 hours (depending on measurement settings)
Storage	Onboard 1 Gbit Flash storage > 25 days of continuous measurement data (3 channels at 2 meas/s each)
Size and weight	Size: (see picture) Weight: approx. 10 g (including battery)

9.4.3 Docking station & Software

Connection to PC	• Micro-USB for data and power • Windows Software for data download
Programming interface	Included in the docking station. Used for logger device programming and firmware updates.
Export format	CSV
System requirements	Windows 7 or newer